

Highlights

Reducing RES Droughts through the integration of wind and PV

Boris Morin, Aina Maimó Far, Damian Flynn, Conor Sweeney

- RES droughts are analysed using 45 years of hourly wind and PV generation data
- RES droughts from C3S-Energy and ERA5-Atlite datasets are compared
- Adding PV to a wind-dominated system reduces RES drought frequency and duration
- Validated RES datasets are crucial to accurately identify RES drought extremes

Reducing RES Droughts through the integration of wind and PV

Boris Morin^{a,*}, Aina Maimó Far^a, Damian Flynn^b, Conor Sweeney^a

*^aSchool of Mathematics and Statistics, University College Dublin, Belfield, Dublin
4, Dublin, D04 V1W8, Ireland*

*^bSchool of Electrical and Electronic Engineering, University College Dublin, Belfield,
Dublin 4, Dublin, D04 V1W8, Ireland*

*Corresponding author

Email addresses: `boris.morin@ucdconnect.ie` (Boris Morin),
`aina.maimofar@ucd.ie` (Aina Maimó Far), `damian.flynn@ucd.ie` (Damian Flynn),
`conor.sweeney@ucd.ie` (Conor Sweeney)

Abstract

Increasing the share of electricity produced from renewable energy sources (RES), combined with RES dependence on weather, poses a critical challenge for energy systems. This study investigates the importance of the balance between wind and photovoltaic (PV) capacity on periods of low renewable generation, known as RES droughts. Three different RES models are used to estimate the capacity factors for different scenarios of installed capacities for wind and PV power. The skill of the RES models is quantified by comparing capacity factor time series to observed hourly data and by assessing their representation of observed RES droughts. The RES models are used to generate a 45-year hourly time series of RES capacity factor, enabling analysis of the frequency, duration and return periods of RES droughts at a climatological scale. Results show the importance of using an accurate, validated RES model for RES drought risk assessment. The addition of PV capacity to a wind-dominated system results in a significant reduction in the frequency and duration of RES droughts, while also reducing extremes and seasonal drought patterns. These findings underscore the importance of diversification in RES capacity to enhance energy security and resilience.

Keywords: RES Drought, Wind Power, Solar PV Power, Renewable Energy Sources, Return Periods

1. Introduction

The EU aims to generate at least 69% of its electricity from renewable energy sources (RES) by 2030, up from 41% in 2022 [1]. While this transition is essential for reducing greenhouse gas emissions, it also highlights the challenge of managing the variability of weather-dependent energy sources such as wind and photovoltaic (PV) power. This challenge is compounded by the increasing electrification of energy sectors, which places greater demand on the power system and makes it more sensitive to meteorological conditions, both in historical [2] and future climates [3]. Periods of low renewable generation, known as *Dunkelflaute* or RES droughts, pose significant risks to system adequacy and energy security, emphasising the need for a resilient energy system to meet both growing electricity demand and decarbonisation targets.

14 This study focuses on Ireland, a region with a strong reliance on wind
15 power, which has ambitious targets for PV power expansion. This case study
16 provides valuable insights into the potential benefits of diversifying the re-
17 newable energy mix on RES droughts. The performance of different RES
18 datasets are compared, and a 45-year time series of RES generation is pro-
19 duced. The results highlight the role of increased PV capacity in reducing
20 RES drought risks, offering insights for policymakers and energy planners.

21 For this study, a RES drought event is defined as occurring when the
22 average capacity factor (CF) remains below a fixed threshold for a given du-
23 ration, following the methodology used in previous research. Kaspar et al. [4]
24 analysed the shortfall risks of low wind and PV in Europe, with a focus on
25 Germany. Mockert et al. [5] expanded on this by examining the link between
26 weather regimes and RES droughts in Germany. Similar analyses were con-
27 ducted using machine learning for Japan [6] and Hungary [7]. Alternative
28 methods exist for defining RES droughts. One approach uses relative CF
29 thresholds that adjust throughout the year to account for seasonal variations
30 in renewable electricity generation. Raynaud et al. [8] defined a drought as
31 a sequence of days with energy production below a threshold, applying this
32 method over a number of European regions. This methodology was later
33 used to study wind and PV droughts in India using machine learning meth-
34 ods [9]. Kapica et al. [10] built upon this approach to compare the likelihood
35 of RES droughts increasing in Europe under different climate models. Ri-
36 naldi et al. [11] instead defined RES droughts as periods when wind or PV
37 CF falls below a percentage of the daily mean for that time of year and as-
38 sessed RES drought risks in the U.S. Western Interconnection. Also focusing
39 on the U.S., Brown et al. [12] used a weekly timescale rather than hourly or
40 daily data and examined RES droughts from a meteorological perspective.
41 Another method defines energy drought indices based on metrics commonly
42 used in hydro-meteorology to characterise RES droughts [13]. This approach
43 identifies periods of unusually low generation relative to historical production
44 levels, using the lowest production percentiles. It has been applied in other
45 studies, including analyses of RES droughts in the U.S. [14] and China [15].

46 In addition to examining periods of low renewable electricity generation,
47 Raynaud et al. [8] analysed the imbalance between electricity demand and
48 renewable generation, known as residual load. These events were studied
49 alongside low-generation periods to assess their correlation. Similar analyses
50 have been conducted in Europe [13] and the U.S. [14], revealing differing
51 results across regions.

52 Additionally, some studies combine these definitions with metrics that
53 incorporate the demand side of energy consumption, analysing the balance
54 between supply and demand during drought periods [8, 11, 13, 14].

55 In this paper, the focus is exclusively on renewable electricity generation,
56 and a fixed threshold approach to define RES droughts is used, which facil-
57 itates consistent inter-comparison between scenarios with different installed
58 wind and PV capacities.

59 RES droughts are identified using onshore wind and PV CF time series.
60 In this study, three different datasets are used, all of which are driven by
61 ERA5 data [16]. Two of the datasets are part of C3S Energy (C3S-E), an
62 energy-based operational dataset produced by the EU Copernicus Climate
63 Change Service [17]. One of the C3S-E datasets provides CF time series
64 aggregated at the national scale, while the other provides the CF time series
65 at each grid point, at the ERA5 resolution of 0.25° . The third dataset was
66 generated using the Atlite model [19], which converts the ERA5 atmospheric
67 data to a generation time series using specified wind turbine and PV panel
68 models. Atlite is an open-source tool developed by PyPSA [19] and has
69 been used for estimating wind and PV generation in order to study RES
70 droughts [5].

71 The datasets used in this study are detailed in section 2, which describes
72 their characteristics and relevance for evaluating RES droughts. Section 3
73 outlines the RES datasets used to simulate wind and PV generation and
74 provides the methodology for defining and identifying RES drought events,
75 including the thresholds and metrics applied. In section 4, the datasets are
76 first verified against observed energy data to assess their accuracy, followed
77 by an analysis of RES drought occurrences for two scenarios with different
78 ratios of installed wind to PV capacities. Finally, section 5 offers a discussion
79 of the results in the context of energy reliability and future planning, followed
80 by the main conclusions and recommendations for further research.

81 2. Data

82 This study uses publicly available datasets to construct and validate the
83 datasets for estimating the CF of wind and PV energy. The primary data
84 sources include: EirGrid and SONI, the transmission system operators (TSO)
85 for the Republic of Ireland and Northern Ireland, respectively; the ERA5
86 reanalysis dataset; and the C3S-E datasets.

87 2.1. Wind and PV Capacity and Availability

88 EirGrid, the TSO for the Republic of Ireland, and SONI, the Northern
89 Ireland TSO, provide detailed datasets on all wind and PV farms across the
90 island of Ireland (Republic of Ireland and Northern Ireland) from 1990 to the
91 present [23]. These datasets include information such as each farm’s installed
92 capacity, name, and connection date. To enhance the accuracy of this data,
93 the longitude and latitude for each farm were manually determined through
94 online searches. For simplicity, this data will be referred to as originating
95 from EirGrid, as all-island data was directly obtained from EirGrid, and the
96 combined regions of the Republic of Ireland and Northern Ireland will be
97 referred to as Ireland throughout the remainder of this document.

98 The spreadsheet available from the EirGrid website contains two key vari-
99 ables: generation and availability. Generation is the energy that a RES farm
100 actually contributed to the grid, which may include limitations introduced
101 by the TSO to maintain grid stability, such as constraints and curtailment.
102 Availability represents the energy that would have been generated from a
103 RES farm if no grid constraints had been applied, making it representative
104 of the weather-related response. Generation and availability values are avail-
105 able from 2014 onward for wind power and from 2018 onward for PV power,
106 although PV availability data only became present in the Republic of Ireland
107 in 2023. This study focuses on availability for all analyses.

108 2.2. Atmospheric Variables

109 Atlite and C3S-E datasets are driven by the ERA5 reanalysis [16], pro-
110 duced by the European Centre for Medium-Range Weather Forecasts (ECMWF).
111 This global gridded dataset provides hourly atmospheric variables from 1940
112 to the present at a horizontal resolution of 0.25° . It is widely used for esti-
113 mating solar and wind energy [5, 17, 12, 24]. Table 1 lists the ERA5 variables
114 used by Atlite and C3S-Energy.

115 2.3. C3S Energy

116 The EU Copernicus Climate Change Service developed the C3S-E renew-
117 able energy dataset for Europe [17], using ERA5 atmospheric variables and
118 weather-to-energy models. This dataset provides hourly CF for wind and PV
119 energy from 1979 to the present. The data are available on the same grid as
120 the ERA5 data, which has a horizontal resolution of 0.25° . The time series
121 are also available for download at two aggregated scales: regional (NUTS 2)
122 and national.

Table 1: ERA5 variables used to calculate wind and PV generation

ERA5 name	variable
100 metre zonal and meridional wind speed	u_{100}, v_{100}
2 metre temperature	$t2m$
Surface net solar radiation	ssr
Surface solar radiation downwards	$ssrd$
Top of atmosphere incident radiation	$tisr$
Total sky direct solar radiation at surface	$fdir$

123 The C3S-E dataset estimates wind energy using wind speeds at 100 me-
 124 tres (u_{100}, v_{100}) and a standard turbine model, the Vestas V136/3450, with
 125 a fixed hub height of 100 meters. This choice is based on expert advice and
 126 the trend in wind turbine installation. The PV generation model used by
 127 C3S-E uses two ERA5 variables: surface solar radiation downwards ($ssrd$)
 128 and air temperature ($t2m$). PV generation is calculated multiple times, us-
 129 ing the same model with different azimuth and tilt angles. The results are
 130 aggregated based on a statistical distribution of the module angles based on
 131 the geographical location [25].

132 3. Methods

133 This study uses three datasets to analyse RES droughts across the island
 134 of Ireland. Data downloaded from C3S-E were used to obtain two datasets:
 135 one based on national-level data (C3S-E N), and another on grid-level data
 136 (C3S-E G). The third dataset was computed using the Atlite model (Atlite).

137 3.1. C3S-Energy National

138 For national-level analyses, the aggregated CF time series provided by
 139 C3S-E were used at two levels: Republic of Ireland (NUTS0: IE) and North-
 140 ern Ireland (NUTS2: UKN0). These are based on the assumption by C3S-E
 141 that RES generation occurs at every ERA5 grid point in Ireland. We com-
 142 puted a weighted average of these, based on the installed capacity of each
 143 one, to represent the total CF for Ireland.

144 3.2. C3S-E Gridded

145 The gridded dataset from C3S-E was used to create CF datasets which
 146 account for the location of RES farms in Ireland. A list of the RES farms in

147 Ireland was compiled, including each farm’s latitude, longitude and installed
148 capacity. Using these coordinates, the nearest grid point on the C3S-E grid
149 was identified for each farm. The CF values from the C3S-E dataset corre-
150 sponding to these grid points were retrieved. A weighted average of the CF
151 values was calculated, with the installed capacity of each farm serving as the
152 weight, to construct the CF time series for Ireland. This process resulted in
153 a time series of RES generation for each energy source (wind and PV) for
154 Ireland, which takes the location of the RES farms into account.

155 3.3. *Atlite*

156 Atlite transforms weather data into energy data using the gridded ERA5
157 data and the locations of existing RES farms, as described in C3S-E G.
158 ERA5 data for wind speed at 100 metres (u_{100} , v_{100}) are used to calculate
159 wind generation, while the ERA5 radiation variables (ssr , $ssrd$, $tisr$, and
160 $fdir$) and air temperature ($t2m$) are used to calculate PV generation. A
161 key distinction between C3S-E and Atlite lies in their representation of wind
162 turbines and PV panels. This study identifies the most appropriate wind
163 turbine power curve to use from the 121 power curves made available by
164 Renewables.ninja [26]. The selection of a specific wind turbine and PV panel
165 characteristics is further discussed and explained in section 4.1.

166 3.4. *Energy Scenarios*

167 In addition to analysing wind and PV generation separately, a combined
168 CF was computed for each dataset by averaging wind and PV generation,
169 weighted by their installed capacities at the end of 2023 (5.9 GW for wind
170 power and 0.6 GW for PV power). This configuration is referred to as the
171 91W-9PV scenario, reflecting the distribution of 91% wind and 9% PV ca-
172 pacity. Given that PV capacity in Ireland is low in 2023, and to explore how
173 a more balanced distribution of wind and PV capacities might impact RES
174 droughts, this study also considered a second scenario, referred to as 57W-
175 43PV, where the installed PV capacity is assumed to increase to 8.6 GW,
176 while wind capacity rises to 11.45 GW. These values are based on targets
177 outlined in the roadmap published by the 2024 Climate Action Plan [27].
178 This study does not include offshore wind in the analysis. Recent reports
179 suggest that even by 2030, Ireland is unlikely to have any significant new off-
180 shore wind farms, with projected offshore capacity expected to remain near
181 zero using realistic scenarios [28].

182 New time series were generated for both the Atlite and C3S-E G PV
 183 datasets, incorporating a revised distribution of installed capacity across Ire-
 184 land as specified in the roadmap. For wind power, the CF time series remains
 185 unchanged, as significant shifts in the location of wind farms are not expected.
 186 In total, twelve CF time series were analysed in this study, six for individual
 187 wind and PV CF (three datasets for each source) in the 91W-9PV scenario,
 188 and an additional six time series that include the combined CF for 91W-9PV
 189 and 57W-43PV scenarios across the different datasets.

190 It is important to note that the specific capacity values used in this study
 191 are illustrative and are not intended to reflect precise future realities. Instead,
 192 they serve to explore the impact of transitioning from a wind-dominated sys-
 193 tem (91W-9PV) to a more evenly distributed system (57W-43PV). This ap-
 194 proach allows for a comparative analysis between the two scenarios, assessing
 195 how the balance of RES capacity affects the occurrence of RES droughts.

196 3.5. *RES Drought Definition*

197 In this study, a RES drought event was defined as occurring when the
 198 24-hour moving average of CF remains below a fixed threshold of 0.1 for
 199 a period of longer than 24 hours. The choice of this threshold is somewhat
 200 arbitrary, but aligns with similar studies on low renewable energy production
 201 [4, 6, 7]. By using a 24-hour moving average, fewer but longer-lasting events
 202 were captured compared to using the raw CF time series, which can be more
 203 sensitive to short-term fluctuations. A fixed threshold approach was chosen
 204 in this study to enable consistent inter-comparison between datasets.

205 The moving average approach smooths out short-term fluctuations, so
 206 that brief periods above the threshold do not interrupt an otherwise con-
 207 tinuous low-CF period (Fig. 1). This means that a single hour above the
 208 threshold does not "break" a drought event if it is surrounded by prolonged
 209 low-generation hours. As a result, fewer but longer-lasting drought events
 210 are identified, which may better reflect real-world conditions where energy
 211 supply constraints persist over extended periods.

212 4. Results

213 4.1. *Verification*

214 The accuracy of the datasets used in this study was verified, before con-
 215 tinuing to the analysis of RES droughts. For the verification process, time-
 216 varying values of installed capacity were used to account for changes in RES

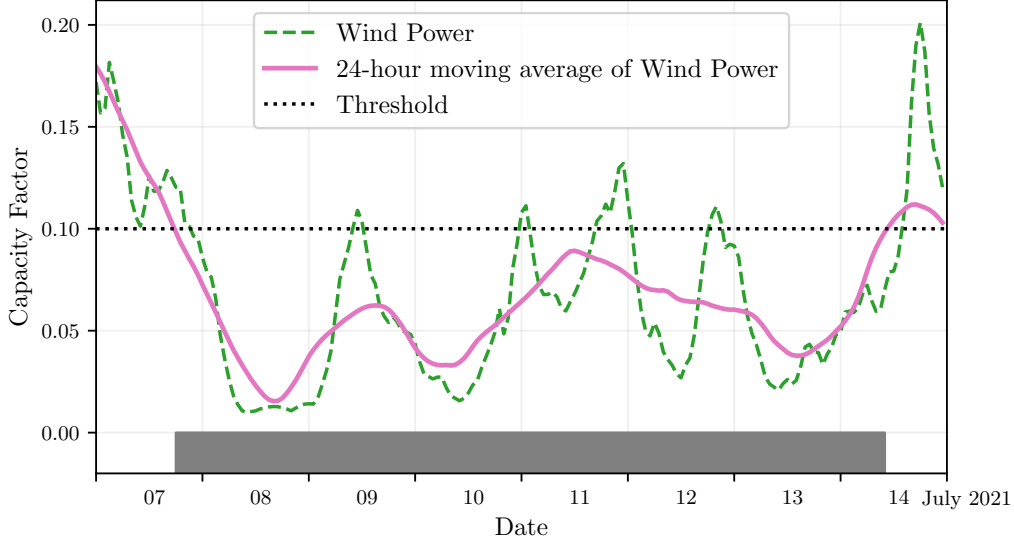


Figure 1: Wind time series of CF (green) and its 24-hour moving average (pink) from the 7th to the 15th of July 2021. The black dashed line indicates the CF threshold. The grey bar shows the period identified as a wind drought under our definition

217 development over the verification period. This step allowed us to assess how
 218 well the datasets represent the production of renewable energy by comparing
 219 them against observed data.

220 4.1.1. Wind Energy

221 The C3S-E datasets use the Vestas V136/3450 wind turbine power curve,
 222 (Fig. 2a). The Atlite model allows the user to specify the power curve.
 223 We considered the 121 power curves available for download from Renew-
 224 ables.ninja [26]. For each power curve, Renewables.ninja also provides four
 225 associated smoothed power curves. The smoothing is done using a Gaussian
 226 filter with different standard deviations that depend on the wind speed. A
 227 separate wind CF time series for Ireland was generated for each of the wind
 228 turbine power curves and smoothing levels.

229 The performance of each CF time series is then assessed based on four skill
 230 scores: correlation coefficient (CC), root mean square error (RMSE), mean
 231 bias error (MBE), and the percentage of overlap. The percentage of overlap
 232 quantifies the similarity between the observed and modelled distributions. It
 233 is a positively oriented skill score, where 100% shows full agreement between

the two distributions, and 0% indicates no overlap. The histograms of hourly
CF values for the most recent decade (2014-2023) are used to calculate this
skill score.

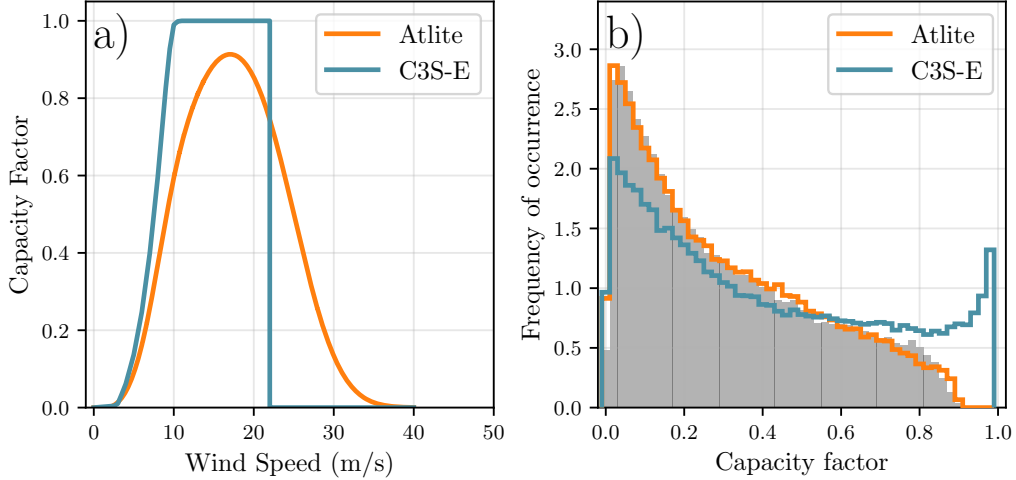


Figure 2: a) Power curves of the Enercon E112.4500 with a $0.3w$ smoothing filter used by Atlite (orange) and the Vestas V136/3450 used by C3S-E (blue) b) Histograms of wind CF for Ireland from Atlite (orange), C3S-E (blue) and Observed (shaded)

Based on these metrics, the most representative power curve for Ireland is the Enercon E112.4500 power curve with the $0.3w$ smoothing filter. The smoothing of the wind turbine power curve represents losses associated with each turbine, as well as losses such as wake effects between turbines, which are important when modelling wind energy on larger spatial scales. The histogram in Fig. 2b shows that the C3S-E power curve tends to underestimate low CF values and overestimate higher ones, whereas the smoothed Atlite power curve more closely follows the observed wind availability data. This is further supported by the percentage of overlap which is higher for Atlite (97.2%) than for C3S-E (83.2%), indicating better agreement with observed data.

The effect of the difference between the power curves is also visible in Fig. 3, which shows a density plot of wind CF values. The two C3S-E datasets are shown to overestimate the observed CF, whereas the Atlite model is in good agreement with the observed data. The skill scores presented in Table 2 show that Atlite performs better than the C3S-E datasets for all of the skill scores.

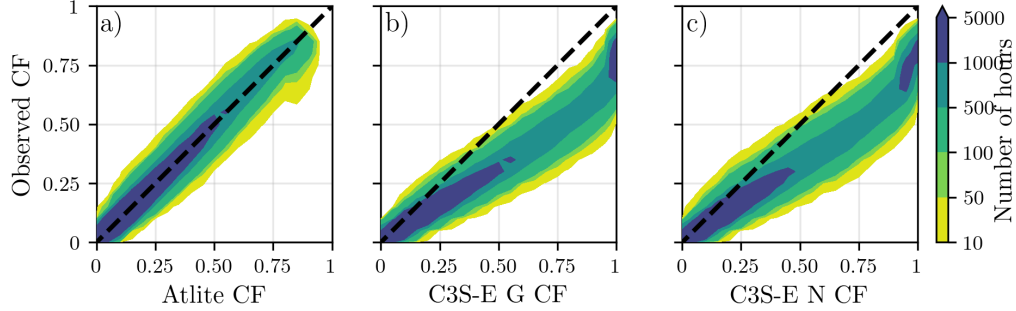


Figure 3: Wind CF density plot of the observed CF (vertical axes) and modelled (horizontal axes) CF data for the a) Atlite, b) C3S-E G and c) C3S-E N datasets

	Atlite	C3S-E G	C3S-E N
CC	0.981	0.972	0.970
RMSE	0.045	0.177	0.162
MBE	-0.003	0.137	0.121

Table 2: Skill scores for wind power for the three datasets compared to observed data

Fig. 4 shows the average annual number of wind drought events during the 2014 to 2023 validation period. The figure reveals that Atlite presents the best overall agreement with the observed frequency and duration of wind drought events. This pattern is particularly evident for shorter-duration events, which are the most frequent.

4.1.2. PV Energy

The Atlite model allows the user to select certain PV panel characteristics. In this study, the three PV panel types available in the Atlite model were considered (CSi, CdTe, Kaneka). Following the same methodology as in the previous section, the three available models were compared using four skill scores (CC, RMSE, MBE, and the percentage of overlap). Based on the best-performing metrics, the Beyer PV panel model was selected [29], using the Kaneka Hybrid panel option. For all PV farm locations, the azimuth angle is fixed at 180°(due south), and the optimal tilt angle option is applied.

The PV installed capacity available on the spreadsheets from EirGrid represents the Maximum Export Capacity (MEC) and does not accurately reflect the installed PV capacity. To enable actual PV generation potential to be modelled correctly, installed capacities were set at 1.4 times the MEC

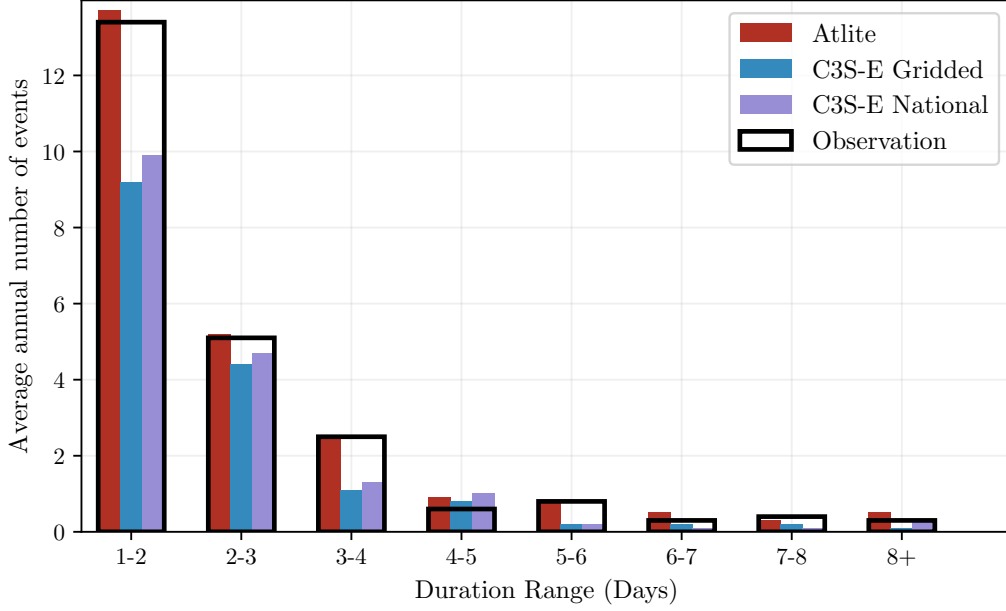


Figure 4: Average annual number of wind drought events for Atlite (red), C3S-E G (blue), C3S-E N (purple), and the observed data (black outline). The wind droughts are identified from 2014 to 2023, considering the actual capacity of the system at any given time

values. This scaling factor was estimated by analysing proprietary data from individual PV farms provided by EirGrid, which showed that, on average, assuming that the installed capacities of farms exceed their MEC values by 40% yields the best agreement with the observed availability.

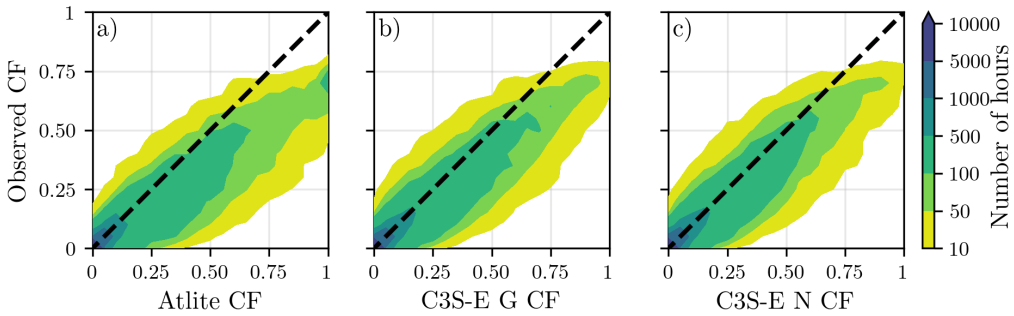


Figure 5: PV CF density plot of the observed (vertical axes) and modelled (horizontal axes) CF series for the a) Atlite, b) C3S-E G and c) C3S-E N datasets

Figure 5 shows that the three datasets have a similar tendency to overestimate the CF compared to the observed values, especially for high CF values. The skill scores presented in Table 3 indicate that C3S-E G performs best overall, with the lowest RMSE and a high correlation coefficient, suggesting a closer match to observed data. All models show a slight positive bias, with Atlite exhibiting a slightly lower correlation and higher RMSE.

	Atlite	C3S-E G	C3S-E N
CC	0.921	0.931	0.931
RMSE	0.119	0.090	0.113
MBE	0.046	0.027	0.021

Table 3: Skill scores for PV CF for the three datasets compared to observed data

Fig. 6 shows the number of PV drought events during the 2023 validation period across different duration ranges. The figure reveals partial agreement between the three datasets and the observed data, with consistent results noticed for duration ranges of 1-2, 3-4, 7-8, and 8+ days. However, discrepancies appear in the other ranges, where the models diverge from the observed data. The main challenge in validating PV data stems from the recent installation of a large share of Ireland’s PV capacity, with over 65% of the total PV capacity installed in 2023. This results in uncertainties in PV generation data and the actual generating capacity in the first few months after each farm is connected.

As the goal of this analysis is to assess the combination of wind and PV generation, the complementary nature of these energy sources mitigates the limitations in PV-only results.

4.2. Analysis

In this section, RES drought events are evaluated under two different scenarios with fixed installed capacities: the 91W-9PV scenario, with 5.9 GW of wind capacity and 0.6 GW of PV capacity; and the 57W-43PV scenario, where wind capacity comprises 11.45 GW and PV capacity increases to 8.6 GW. Both scenarios were driven by 45 years of ERA5 data. Using the RES drought identification process described in Section 3.5, wind and PV droughts are first analysed separately before presenting the results for combined (wind + PV) RES droughts under both scenarios.

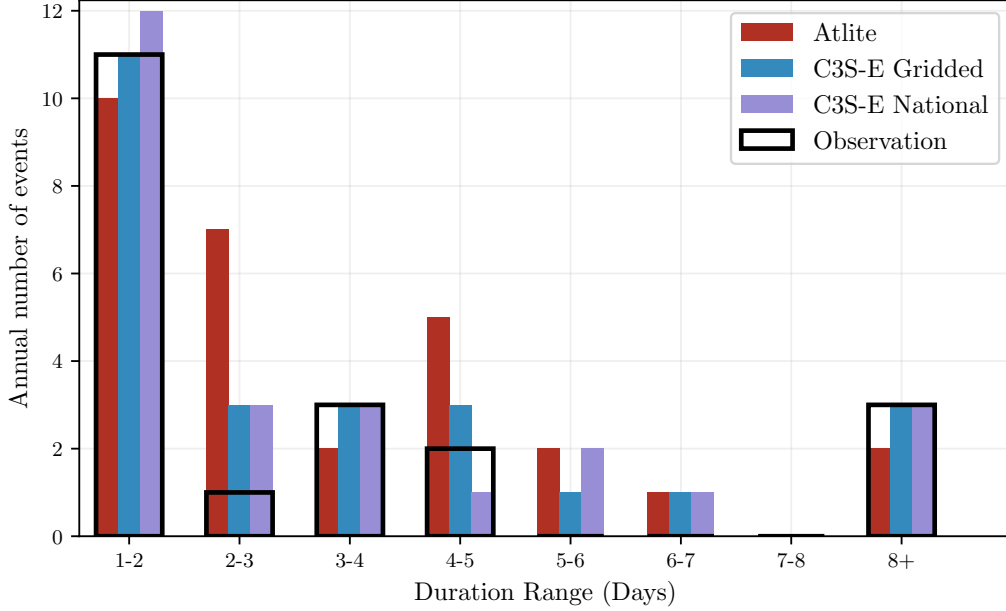


Figure 6: Number of PV drought events for Atlite (red), C3S-E G (blue), and C3S-E N (purple) and the observed data (black outline). The PV droughts are identified for 2023, considering the actual capacity of the system at any given time

4.2.1. Annual Number of RES Droughts

The first part of the analysis examines the annual number of RES drought events across the three datasets. When only wind energy is considered (Fig. 7a), the number of events decreases as the duration range increases, with very few events lasting more than seven days. In the case of only PV energy (Fig. 7b), the number of events also declines as the duration range extends from one to eight days, followed by a slight increase for longer durations. This increase occurs because Ireland, being located above the 50° parallel, experiences reduced sunlight during the winter months. From November to March, PV output often remains consistently low, leading to extended periods where generation stays below the CF threshold.

When comparing wind and PV results (Fig. 7a & b), the median, first, and third quartiles for PV are consistently higher than or equal to those for wind, across all duration ranges and datasets. This is due to the typically lower CF of PV power compared to wind power, especially in a region such as Ireland where solar potential is limited. PV generation is also zero at

night and constrained by the daily solar cycle, leading to a naturally higher frequency of drought events in PV compared to wind.

Fig. 7c & d show the combination of wind and PV under the two capacity scenarios. In the 91W-9PV scenario (Fig. 7c), the identified RES droughts closely match those for wind alone, which is expected due to the dominance of installed wind capacity. In contrast, the 57W-43PV scenario (Fig. 7d) shows a clear reduction in the number of drought events across all datasets and durations, with a decrease of the total number of events of 56% for Atlite, 52% for C3S-E G, and 50% for C3S-E N. This reduction is attributed to the anti-correlation between wind and PV generation.

The median, first, and third quartiles for the Atlite dataset are consistently greater than or equal to those of the other two datasets, regardless of the duration range or type of renewable energy considered. This difference arises from the wind turbine power curve model used in the C3S-E datasets, which tends to overestimate the wind CF (Fig. 3). As a result, the overall number of RES droughts is underestimated in the C3S-E datasets compared to Atlite.

4.2.2. Return Periods of RES Drought Duration

The RES drought events identified over the 45-year period were used to calculate the return periods for different RES drought durations. A return period is the estimated average time interval between events of a specified duration or intensity (not to be confused with the frequency of their occurrence within a fixed time frame). Fig. 8 illustrates the return periods for varying RES drought durations, highlighting how often different drought lengths are likely to occur across the datasets. This analysis provides insight into the frequency and likelihood of prolonged low-generation periods, which is crucial for evaluating the potential impact of RES droughts on energy reliability and security of supply.

The duration of wind droughts (Fig. 8a) increases in a log-linear fashion across the three datasets. The log-linear trend indicates a predictable relationship between drought duration and occurrence, with longer wind droughts becoming exponentially less likely as duration increases.

In the case of PV droughts (Fig. 8b), Atlite behaves differently than the two C3S-E datasets. The Atlite results show a generally log-linear increase. For C3S-E G and C3S-E N, the duration of PV droughts increases in a log-linear pattern for events lasting less than 16 days. Beyond this duration, there is a sharp rise in drought duration for events up to a one-year return

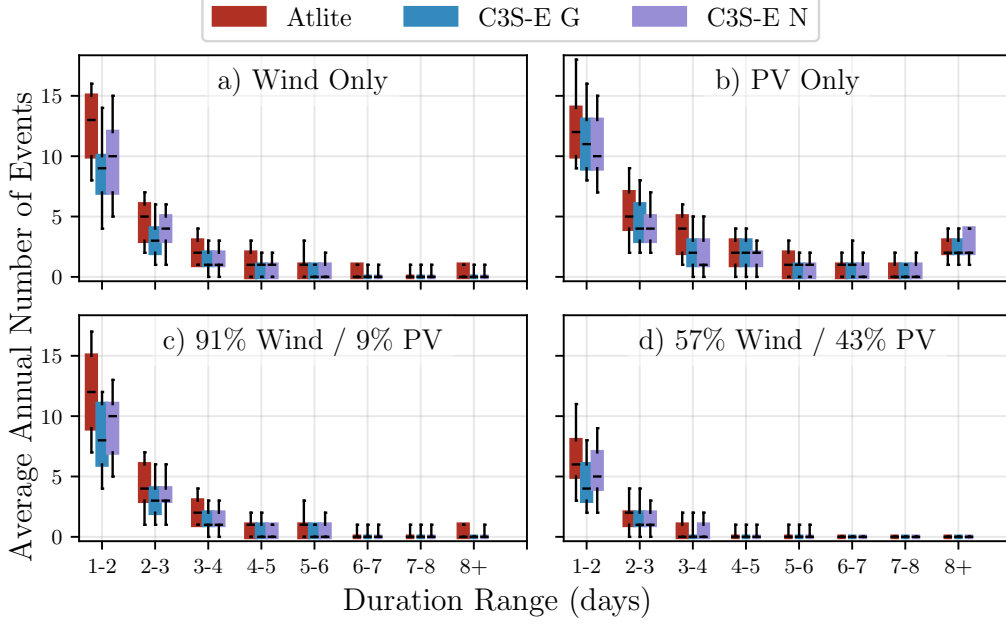


Figure 7: Average annual number of RES droughts (from 1979 to 2023) for a) Wind, b) PV, c) 91W-9PV and d) 57W-43PV for Atlite (red), C3S-E G (blue), and C3S-E N (purple). The x-axis represents duration ranges in days (lower bound included), while the y-axis indicates the annual number of events. The boxes display the first and third quartiles and the median is marked by a black line. The whiskers indicate the 5th and 95th percentiles

period. This sudden increase again reflects the impact of extended periods of low PV generation during winter in Ireland.

The difference between Atlite and the C3S-E results arises from differences in the datasets near the threshold of 0.1 CF. Atlite remains slightly above the threshold more frequently during these conditions, leading to shorter, more fragmented drought events. In contrast, C3S-E G and C3S-E N tend to fall below the threshold in similar conditions, resulting in longer continuous drought periods, especially during winter.

For the 91W-9PV scenario (Fig. 8c), the return periods mirror those of Fig. 8a, due to the low levels of installed PV capacity. In the 57W-43PV scenario (Fig. 8d), the return periods for RES droughts increase across all durations. For example, the return period for a five-day drought event (shown by the vertical dashed lines in Fig. 8) extends from roughly six months for the 91W-9PV scenario, to four years for the 57W-43PV scenario in the Atlite

dataset, and from about fifteen months to around five years in the two C3S-E
 datasets.

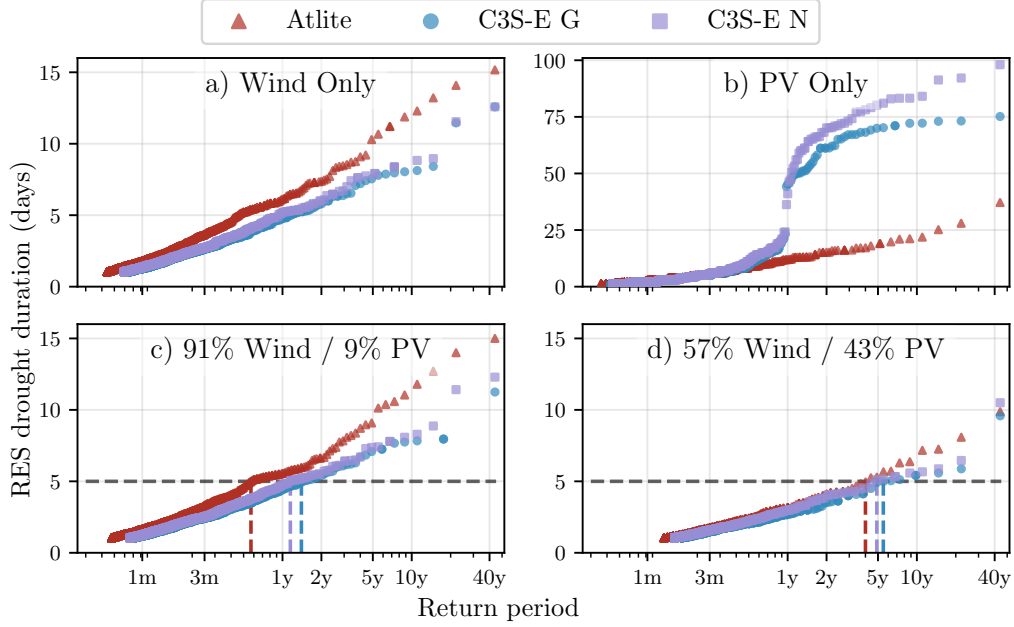


Figure 8: Return periods of the duration of RES droughts (from 1979 to 2023) for a) Wind, b) PV, c) 91W-9PV and d) 57W-43PV for Atlite (red triangle), C3S-E G (blue circle), and C3S-E N (purple square). The x-axis represents the return period time in a log-scale and the y-axis indicates the duration of RES drought associated with it. The horizontal dashed line marks the 5-day return period, with coloured vertical dashed marking its return period for each dataset

Across Fig. 8a, c, and, d, the return periods in the Atlite dataset are
 consistently higher than those in the two C3S-E datasets. For instance, in
 the 91W-9PV scenario (Fig. 8c), an event with a one-year return period
 lasts six days in the Atlite dataset, compared to only five days in the C3S-E
 datasets. This difference underscores the importance of model selection when
 quantifying RES droughts, as each model’s assumptions and parametrisations
 significantly influence drought duration estimates. Additionally, in all four
 graphs, the similarity between results from the two C3S-E datasets suggests
 that assumptions in the Atlite model—such as wind turbine power curve
 selection and PV panel specifications—have a greater impact on RES drought
 duration estimates than the precise geographic distribution of RES farms

384 when studying the return periods of RES droughts.

385 4.2.3. Seasonal Distribution of RES Droughts

386 The seasonality of RES droughts was analysed by comparing the percent-
387 age of hours in each month classified as part of a RES drought.

388 For wind-dominated scenarios (Fig. 9a & c), the percentage of hours that
389 are part of a drought is higher in summer than in winter. In the Atlite
390 dataset, for instance, an average of 24% of hours in summer (June-July-
391 August) are identified as wind droughts, compared to only 4% in winter
392 (December-January-February). This seasonal variation is less prominent for
393 the two C3S-E datasets compared to the Atlite one. This difference can be
394 linked to the shape of the two power curves (Fig. 2). CFs near or under the
395 0.1 threshold occur at higher wind speeds for the Atlite power curve than
396 for the C3S-E one. In contrast, the results for PV droughts (Fig. 9b) show
397 a higher percentage in winter, with PV droughts occurring over 60% of the
398 time regardless of the dataset. The Atlite results show a higher percentage of
399 PV drought hours for wind, and a slightly lower percentage for PV, compared
400 to the two C3S-E datasets.

401 The 91W-9PV scenario (Fig. 9c) shows patterns comparable to the ones
402 for wind droughts (Fig. 9a). However, in the 91W/9PV scenario, the number
403 of hours classified as RES droughts in summer decreases slightly compared to
404 the wind-only scenario. This reduction can be explained by the contribution
405 of PV generation during the summer months in the 91W-9PV scenario, even
406 though it constitutes only 11% of total capacity. Since the number of RES
407 drought hours for PV in summer is near zero, this small contribution has a
408 noticeable impact on reducing overall drought hours. In the 57W-43PV sce-
409 nario (Fig. 9d), all three datasets show a reduction in monthly RES drought
410 frequency. Annual reductions in median RES drought frequency are observed
411 across the datasets, dropping from 14% to 5% for Atlite, from 8% to 3% for
412 C3S-E G, and from 9% to 4% for C3S-E N. The balanced mix of wind and
413 PV power in this scenario reduces the seasonal signal overall and significantly
414 decreases the percentage of RES drought hours in the summer.

415 5. Discussion and Conclusions

416 This study has investigated the ability of three RES datasets to repre-
417 sent RES droughts: Atlite, C3S-E G, and C3S-E N. One of the most evident
418 differences is how each dataset incorporates the specific locations of RES

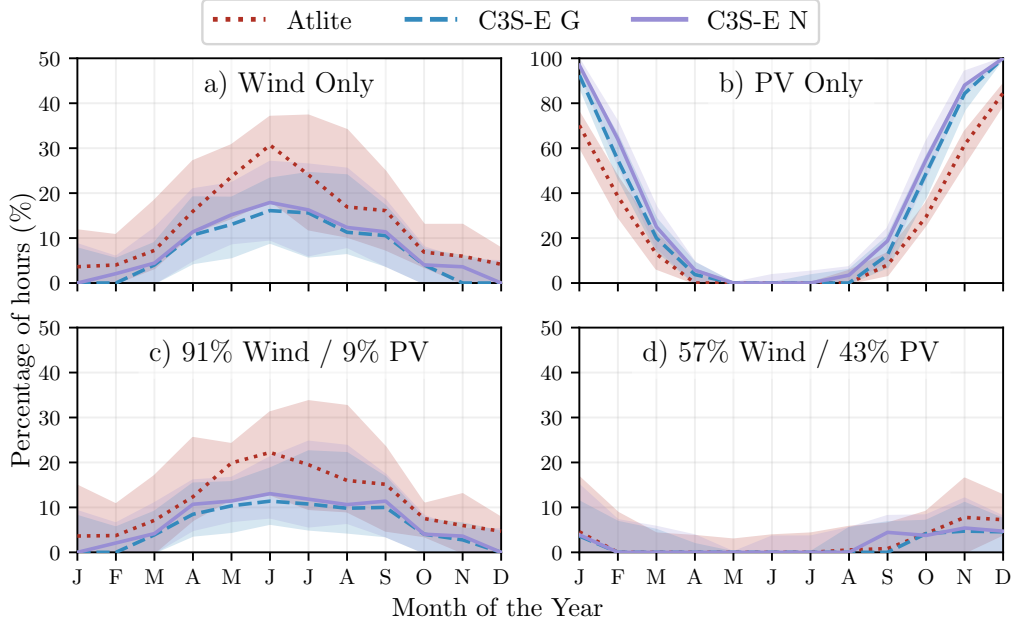


Figure 9: Percentage of hours in a month which are part of a RES drought (from 1979 to 2023) for a) Wind, b) PV, c) 91W-9PV and d) 57W-43PV for Atlite (red dotted), C3S-E G (blue dashed), and C3S-E N (purple solid). The x-axis represents the month of the year, and the y-axis indicates the percentage of hours. Lines correspond to the median values and the area between the first and third quartiles is shaded. Note the different y-axis scale for b).

419 farms. Both Atlite and C3S-E G consider the locations of wind and PV
 420 farms, which one would expect to result in a more accurate representation
 421 of RES generation. While this approach slightly improves PV models, our
 422 analysis indicates that for wind energy, the Atlite dataset performs better
 423 overall, especially in its close alignment with observed data for wind gener-
 424 ation estimates. This finding suggests that, although the inclusion of RES
 425 farm locations is beneficial, the accuracy of the RES dataset is more strongly
 426 influenced by underlying model assumptions, such as selecting an appropriate
 427 wind power curve.

428 Atlite shows the best alignment with observed data for wind generation.
 429 Differences between the datasets are smaller for PV, with C3S-G perform-
 430 ing marginally better than the other two. The results show that the two
 431 C3S-E datasets (C3S-E G and C3S-E N) consistently yield similar outcomes,

432 indicating that their methodological differences have minimal impact in this
433 case. This distinction is also evident in the analysis, where Atlite reports
434 higher return periods and a greater number of RES droughts, especially in
435 scenarios with a balanced share of RES. Again, the results from RES drought
436 modelling rely more on the precision of the wind power curve and PV panel
437 models than on the specific locations of RES farms. Atlite’s superior perfor-
438 mance highlights the importance of selecting validated models for assessing
439 RES drought risks. This careful model selection can better quantify risks,
440 support effective planning, and avoid the potential underestimation of ca-
441 pacity needs, which is essential for ensuring energy security.

442 Looking at the 57W-43PV scenario, the analysis showed a significant im-
443 provement in the management of RES droughts due to the complementary
444 nature of wind and PV generation. Wind and PV together perform better
445 in terms of reducing drought frequency and duration than either would in-
446 dividually, largely because of the seasonal anti-correlation between the two
447 energy sources. This diversification reduces the seasonal impact on RES
448 droughts, as PV generation peaks in the summer and wind generation is
449 more consistent in winter. Ireland currently has a highly wind-dependent
450 energy system, but with ambitious targets for PV installations in the coming
451 years, the energy mix is expected to approach a balance between wind and
452 PV capacity. While this balanced approach offers a more stable and secure
453 energy supply by mitigating RES drought risks, it is important to note that
454 having similar wind and PV capacities may not optimise other aspects, such
455 as annual energy production or meeting nighttime loads. For policymakers,
456 these findings underscore the importance of meeting these capacity targets
457 to enhance energy security through diversification. Additionally, the choice
458 of model for RES drought assessment becomes increasingly critical as more
459 renewable capacity is integrated into the system.

460 Future work is planned to extend the current analysis. First, climate
461 projection data will be integrated with different energy scenarios, incorpo-
462 rating the addition of offshore wind, to better understand how climate change
463 might affect RES droughts. Second, expanding the geographic domain of the
464 study to include the rest of Europe would provide a more comprehensive un-
465 derstanding of RES droughts in an interconnected energy grid. This would
466 require extensive verification across other European countries, making it a
467 more complex but highly relevant challenge.

468 Data Availability

469 The ERA5 data can be obtained from the Climate Data Store (<https://doi.org/10.24381/cds.adbb2d47>). The C3S-E dataset is also available
470 from the Climate Data Store (<https://doi.org/10.24381/cds.4bd77450>).
471 Information on wind and PV farms in Ireland can be obtained from the
472 EirGrid website ([https://www.eirgrid.ie/grid/system-and-renewable](https://www.eirgrid.ie/grid/system-and-renewable-data-reports)
473 [-data-reports](https://www.eirgrid.ie/grid/system-and-renewable-data-reports)). The Atlite model used in this study is open-source and can
474 be found on GitHub (<https://github.com/pypsa/atlite>). The data and
475 code required to reproduce the analysis in this article will be made available
476 upon acceptance of the manuscript in a public GitHub repository.
477

478 Acknowledgments

479 The research conducted in this publication was funded by Science Foun-
480 dation Ireland and co-funding partners under grant number 21/SPP/3756
481 through the NexSys Strategic Partnership Programme.

482 References

- 483 [1] EuroStat, Renewable Energy Statistics, 2023. URL: [https://ec.europa.eu/eurostat/statistics-explained/index.php?title=Renewable](https://ec.europa.eu/eurostat/statistics-explained/index.php?title=Renewable_energy_statistics)
484 [energy_statistics](https://ec.europa.eu/eurostat/statistics-explained/index.php?title=Renewable_energy_statistics), Accessed: 2024-11-06.
485
- 486 [2] H. C. Bloomfield, D. J. Brayshaw, L. C. Shaffrey, P. J. Coker, H. E.
487 Thornton, Quantifying the increasing sensitivity of power systems to
488 climate variability, *Environmental Research Letters* 11 (2016) 124025.
489 doi:10.1088/1748-9326/11/12/124025.
- 490 [3] H. C. Bloomfield, D. J. Brayshaw, A. Troccoli, C. M. Goodess, M. De Fe-
491 lice, L. Dubus, P. E. Bett, Y.-M. Saint-Drenan, Quantifying the
492 sensitivity of european power systems to energy scenarios and cli-
493 mate change projections, *Renewable Energy* 164 (2021) 1062–1075.
494 doi:10.1016/j.renene.2020.09.125.
- 495 [4] F. Kaspar, M. Borsche, U. Pfeifroth, J. Trentmann, J. Drücke, P. Becker,
496 A climatological assessment of balancing effects and shortfall risks of
497 photovoltaics and wind energy in germany and europe, *Advances in*
498 *Science and Research* 16 (2019) 119–128. doi:10.5194/asr-16-119-2
499 019.

- 500 [5] F. Mockert, C. M. Grams, T. Brown, F. Neumann, Meteorological
501 conditions during periods of low wind speed and insolation in Germany:
502 The role of weather regimes, Meteorological Applications 30 (2023)
503 e2141. doi:10.1002/met.2141.
- 504 [6] M. Ohba, Y. Kanno, D. Nohara, Climatology of dark doldrums in japan,
505 Renewable and Sustainable Energy Reviews 155 (2022) 111927. doi:10
506 .1016/j.rser.2021.111927.
- 507 [7] M. J. Mayer, B. Biró, B. Szücs, A. Aszódi, Probabilistic modeling of
508 future electricity systems with high renewable energy penetration using
509 machine learning, Applied Energy 336 (2023) 120801. doi:10.1016/j.
510 apenergy.2023.120801.
- 511 [8] D. Raynaud, B. Hingray, B. François, J. Creutin, Energy droughts from
512 variable renewable energy sources in European climates, Renewable
513 Energy 125 (2018) 578–589. doi:[https://doi.org/10.1016/j.renene](https://doi.org/10.1016/j.renene.2018.02.130)
514 .2018.02.130.
- 515 [9] A. Gangopadhyay, A. K. Seshadri, N. J. Sparks, R. Toumi, The role
516 of wind-solar hybrid plants in mitigating renewable energy-droughts,
517 Renewable Energy 194 (2022) 926–937. doi:10.1016/j.renene.2022.
518 05.122.
- 519 [10] J. Kapica, J. Jurasz, F. A. Canales, H. Bloomfield, M. Guezgouz,
520 M. De Felice, Z. Kobus, The potential impact of climate change on
521 european renewable energy droughts, Renewable and Sustainable En-
522 ergy Reviews 189 (2024) 114011. doi:10.1016/j.rser.2023.114011.
- 523 [11] K. Z. Rinaldi, J. A. Dowling, T. H. Ruggles, K. Caldeira, N. S. Lewis,
524 Wind and Solar Resource Droughts in California Highlight the Benefits
525 of Long-Term Storage and Integration with the Western Interconnect,
526 Environmental Science and Technology 55 (2021) 6214–6226. doi:10.1
527 021/acs.est.0c07848.
- 528 [12] P. T. Brown, D. J. Farnham, K. Caldeira, Meteorology and climatology
529 of historical weekly wind and solar power resource droughts over western
530 North America in ERA5, SN Applied Sciences 3 (2021) 814. doi:10.1
531 007/s42452-021-04794-z.

- 532 [13] S. Allen, N. Otero, Standardised indices to monitor energy droughts,
533 Renewable Energy 217 (2023) 119206. doi:10.1016/j.renene.2023.11
534 9206.
- 535 [14] C. Bracken, N. Voisin, C. D. Burleyson, A. M. Campbell, Z. J. Hou,
536 D. Broman, Standardized benchmark of historical compound wind and
537 solar energy droughts across the Continental United States, Renewable
538 Energy 220 (2024) 119550. doi:https://doi.org/10.1016/j.renene
539 .2023.119550.
- 540 [15] H. Lei, P. Liu, Q. Cheng, H. Xu, W. Liu, Y. Zheng, X. Chen, Y. Zhou,
541 Frequency, duration, severity of energy drought and its propagation in
542 hydro-wind-photovoltaic complementary systems, Renewable Energy
543 (2024) 120845. doi:10.1016/j.renene.2024.120845, 2.
- 544 [16] H. Hersbach, B. Bell, P. Berrisford, S. Hirahara, A. Horányi, J. Muñoz-
545 Sabater, J. Nicolas, C. Peubey, R. Radu, D. Schepers, et al., The ERA5
546 global reanalysis, Quarterly Journal of the Royal Meteorological Society
547 146 (2020) 1999–2049. doi:10.1002/qj.3803.
- 548 [17] L. Dubus, Y. Saint-Drenan, A. Troccoli, M. De Felice, Y. Moreau, L. Ho-
549 Tran, C. Goodess, R. Amaro E Silva, L. Sanger, C3S Energy: A climate
550 service for the provision of power supply and demand indicators for Eu-
551 rope based on the ERA5 reanalysis and ENTSO-E data, Meteorological
552 Applications 30 (2023) e2145. doi:10.1002/met.2145.
- 553 [18] Copernicus Climate Change Service (C3S), Climate and energy indi-
554 cators for Europe from 1979 to present derived from reanalysis., 2020.
555 doi:10.24381/cds.4bd77450, accessed on 28-11-2024.
- 556 [19] F. Hofmann, J. Hampp, F. Neumann, T. Brown, J. Hörsch, Atlite: a
557 lightweight Python package for calculating renewable power potentials
558 and time series, Journal of Open Source Software 6 (2021) 3294. doi:10
559 .21105/joss.03294.
- 560 [20] J. Li, Z. Zhao, D. Xu, P. Li, Y. Liu, M. A. Mahmud, D. Chen, The
561 potential assessment of pump hydro energy storage to reduce renewable
562 curtailment and CO2 emissions in Northwest China, Renewable Energy
563 212 (2023) 82–96. doi:10.1016/j.renene.2023.04.132.

- 564 [21] M. Parzen, H. Abdel-Khalek, E. Fedotova, M. Mahmood, M. M. Frysz-
565 tacki, J. Hampp, L. Franken, L. Schumm, F. Neumann, D. Poli,
566 et al., Pypsa-earth. a new global open energy system optimization
567 model demonstrated in africa, *Applied Energy* 341 (2023) 121096.
568 doi:10.1016/j.apenergy.2023.121096.
- 569 [22] K. Ali Khan Niazi, M. Victoria, Comparative analysis of photovoltaic
570 configurations for agrivoltaic systems in europe, *Progress in Photo-*
571 *voltatics: Research and Applications* 31 (2023) 1101–1113. doi:10.1002/
572 pip.3727.
- 573 [23] EirGrid & SONI, System and Renewable Data Reports, 2023. URL:
574 [https://www.eirgrid.ie/grid/system-and-renewable-data-rep-](https://www.eirgrid.ie/grid/system-and-renewable-data-reports)
575 [orts](https://www.eirgrid.ie/grid/system-and-renewable-data-reports), Accessed: 2024-11-06.
- 576 [24] N. Otero, O. Martius, S. Allen, H. Bloomfield, B. Schaeffli, Character-
577 izing renewable energy compound events across Europe using a logistic
578 regression-based approach, *Meteorological Applications* 29 (2022) e2089.
579 doi:10.1002/met.2089, 13.
- 580 [25] Y.-M. Saint-Drenan, L. Wald, T. Ranchin, L. Dubus, A. Troccoli, An
581 approach for the estimation of the aggregated photovoltaic power gener-
582 ated in several European countries from meteorological data, *Advances*
583 *in Science and Research* 15 (2018) 51–62. doi:10.5194/asr-15-51-201
584 8.
- 585 [26] I. Staffell, S. Pfenninger, Using bias-corrected reanalysis to simulate
586 current and future wind power output, *Energy* 114 (2016) 1224–1239.
587 doi:10.1016/j.energy.2016.08.068.
- 588 [27] Gouvernement of Ireland, Climate Action Plan 2024, Technical Report 3,
589 Department of the Environment, Climate and Communications, 2023.
590 URL: [https://www.gov.ie/pdf/?file=https://assets.gov.ie/](https://www.gov.ie/pdf/?file=https://assets.gov.ie/284675/70922dc5-1480-4c2e-830e-295afd0b5356.pdf)
591 [284675/70922dc5-1480-4c2e-830e-295afd0b5356.pdf](https://www.gov.ie/pdf/?file=https://assets.gov.ie/284675/70922dc5-1480-4c2e-830e-295afd0b5356.pdf), Accessed:
592 2024-11-06.
- 593 [28] Sustainable Energy Authority Ireland, National Energy Projections
594 2024, Technical Report, Sustainability Energy Authority of Ireland,
595 2024. URL: [https://www.seai.ie/news-and-events/news/energ](https://www.seai.ie/news-and-events/news/energy-projections-report)
596 [y-projections-report](https://www.seai.ie/news-and-events/news/energy-projections-report), Accessed: 2024-11-06.

- 597 [29] H. G. Beyer, G. Heilscher, S. Bofinger, A robust model for the mpp
598 performance of different types of pv-modules applied for the performance
599 check of grid connected systems, Eurosun (2004) 8.